

# Monodisperse carbon nanopearls in a foam-like arrangement: a new carbon nano-compound for cold cathodes

A. Levesque<sup>a</sup>, Vu Thien Binh<sup>a,\*</sup>, V. Semet<sup>a</sup>, D. Guillot<sup>a</sup>, R.Y. Fillit<sup>b</sup>,  
M.D. Brookes<sup>c</sup>, T.P. Nguyen<sup>d</sup>

<sup>a</sup>Equipe Emission Electronique, LPMC-CNRS, Université Lyon 1, Villeurbanne 69622 France

<sup>b</sup>Ecole Nationale Supérieure des Mines, PECM CNRS, 42023 Saint Etienne, France

<sup>c</sup>Defence Science and Technology Laboratory, Fort Halstead, Kent TN14 7BP, UK

<sup>d</sup>Laboratoire de Physique Cristalline, IMN, 44322 Nantes, France

Available online 28 July 2004

## Abstract

This paper reports the low cost, high yield chemical vapor deposition synthesis of a potentially novel carbon nanomaterial using nickel nanocluster-catalysed dissociation of acetylene at 700 °C. The resulting ‘carbon nanopearls’ are 150 nm in diameter with ~ 85% monodispersity, with a solid structure composed of both amorphous and nanocrystalline (~ 2 nm repeat unit) regions. The nanopearls form 3D space-filling ‘strings’ which give rise to a macroscopic foam-like appearance. The nanopearls have been characterized using scanning electron microscopy, high resolution transmission electron microscopy, X-ray microdiffraction, Raman spectroscopy and energy dispersive X-rays. A mechanism for the formation of the nanopearls is proposed based on concentric layers of ~ 4 × 4 nm graphitic flakes. The small radius of curvature of each nanopearl and the corrugation at the atomic scale of the surface resulting from the unclosed graphitic flakes result in excellent field emission properties. It has been demonstrated that a film of conditioned carbon nanopearls exhibits Fowler–Nordheim field emission behavior, with currents of up to 50 μA readily obtainable under continuous emission in moderate vacuum. It is proposed that such emitters would provide significantly higher yield, uniform emission characteristics than non-oriented films of carbon nanotubes due to the reproducibly high density of nanopearl emitter sites.

© 2004 Elsevier B.V. All rights reserved.

PACS: 81.05.Zx; 81.15.Gh; 81.07.Wx; 85.45.Db

Keywords: Carbon nanopearls; Carbon nanospheres; Field emission; Cold cathodes; Chemical vapor deposition growth

## 1. Introduction

Cold electron generation via field emission (FE) is a key technology for the development of many diverse applications in vacuum microelectronics, ranging from space thrusters to miniaturized X-ray and radio-frequency generators, to flat panel displays. The early potential of Spindt tips, 3D microfabricated metallic emitters, was not realized because of problems relating not only to the cost of manufacturing (due to the poor yield), but also to emission

instabilities and non-uniformity resulting from aging-induced surface modifications of the metallic tips.

The quest to develop improved and lower-cost cold emitters therefore started in earnest and led to the emission characterization of carbon nanotubes (CNTs), which represent the current benchmark for cost-effective field emitters. However, CNTs pose problems of their own: the tubular structure of the CNT confines the field emission to the apex region, and therefore layered films of CNTs, which are inexpensive to deposit, suffer from considerable non-uniformity of emission. The solution to this problem is the much more expensive and time-consuming growth of parallel arrays of individual, ‘stand-alone’ CNTs perpendicular to the substrate surface, adding significantly to the cost of fabrication of large displays and electron sources. Neverthe-

\* Corresponding author. Tel.: +33-472-44-80-70; fax: +33-472-44-82-45

E-mail address: [vuthien@lpmcn.univ-lyon1.fr](mailto:vuthien@lpmcn.univ-lyon1.fr) (V.T. Binh).

less, CNTs are otherwise excellent field emitters, demonstrating stable emission characteristics under poor vacuum conditions due to the properties of the graphene surface structure of the apex region.

Carbon is a very versatile material that can form various structures such as diamond films, fullerenes (C<sub>60</sub> and its family) and CNTs. The variety of the structures produced by carbon are a consequence of its stable C–C bonds arising from sp<sup>2</sup> (graphene) and sp<sup>3</sup> (diamond) orbital hybridization. Depending on the growth conditions, the sp<sup>2</sup> carbon atoms can form pentagonal and heptagonal carbon rings that, in combination with the less strained and therefore more thermodynamically favorable hexagonal carbon rings, can produce a large variety of geometrical configurations. These can range from nano- to micron-sized spheres, which may be solid or hollow, amorphous or with onion-like layers, to CNTs having single or multi-walled configurations [1].

This paper reports the synthesis and FE properties of a novel cost-effective carbon nanomaterial, ‘carbon nanopearls’, monodisperse solid 150 nm diameter nanospheres of nanocrystalline carbon that form continuous 3D chains analogous to strings of pearls. The principal advantage of carbon nanopearls is that they are readily produced and unlike CNTs do not require structural orientation for stable and uniform field emission. Section 2 describes the chemical vapor deposition (CVD) process for the fabrication of the carbon nanopearls. Section 3 presents the physical characterization of the nanopearls using different complementary analytical techniques (scanning electron microscopy

(S.E.M.), high resolution transmission electron microscopy (HRTEM), micro X-ray diffraction, Raman, energy-dispersive X-rays (EDX) and Fresnel projection microscopy (FPM). Section 4 proposes a growth mechanism for these graphitic carbon nanospheres. Section 5 reports the FE properties obtained from cold cathodes using these carbon nanopearls and Section 6 presents the conclusions.

## 2. CVD growth process of carbon nanopearls

To our knowledge, at least two different techniques for obtaining monodisperse solid carbon spheres or beads have been reported in the literature. Wang and Kang [2] reported the synthesis of carbon nanospheres by decomposition of CH<sub>4</sub> at 1100 °C with mixed-valent (rare earth metal) oxide-catalytic carbonization (MVOCC). The use of oxides as catalysts was cited as the key to MVOCC. These carbon spheres had an average diameter of 210 nm and monodispersity of 85.7% and were formed on the wall of the reaction chamber. These smooth, non-porous solid spheres were composed of partially ordered graphitic flakes in the size range 1–30 nm, and were dispersive with no aggregation. Sharon et al. [3] reported the synthesis of ‘spongy carbon nanobeads’ by means of pyrolysing camphor vapor at 1000 °C in an argon atmosphere, using ferrocene as a catalyst. Both solid and hollow carbon nanobeads were formed of two sizes, ~ 250 nm and 500–800 nm, and these were composed of amorphous layers

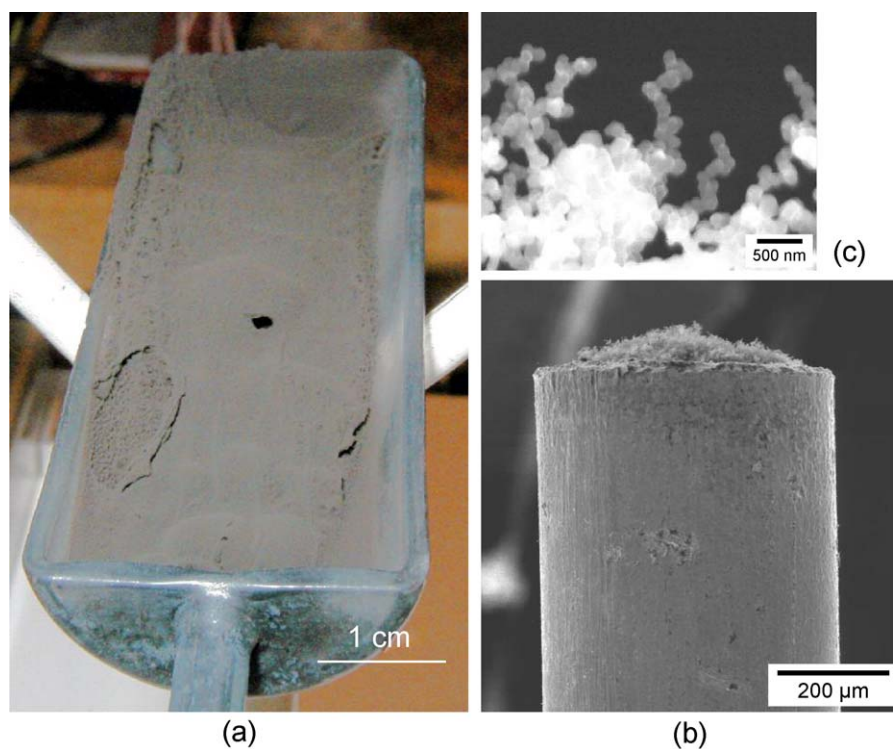


Fig. 1. (a) Volumetric foam-like structure of the carbon nanopearls. (b) Direct localized deposition of the foam-like arrangement of carbon nanopearls at the end of a metallic wire, to be used as cold cathode (S.E.M. image). (c) Side view of the surface of the nanopearl layer of (b) (S.E.M. image).

covered by graphitic shells. They observed aggregation of the larger beads with 10 or more being interconnected by an outer shell and an outer covering of fibrous graphitic carbon.

The new technique [4] reported here produces strings of carbon nanopearls at very low cost, at a temperature of only 700 °C, with Ni clusters as catalysts and giving high yields of virtually monodispersed, 150 nm diameter solid carbon spheres linked in long continuous strings to form a 3D foam-like macroscopic structure. The CVD synthesis uses a mixture of acetylene (as the source of carbon) and nitrogen (20% C<sub>2</sub>H<sub>2</sub>, 80% N<sub>2</sub>). This gas mixture flowed through a quartz tube (80 sccm (C<sub>2</sub>H<sub>2</sub>)/400 sccm (N<sub>2</sub>)), in which Ni clusters having a diameter of around 100 nm had been placed in a reaction vessel. The nanoclusters of Ni were obtained from a sol–gel process followed by a mechanical filtration to obtain a good monodispersity in the size of the Ni clusters.

The formation of the carbon nanopearls was found to be temperature-controlled. Whereas at 600 °C, the Ni nanoclusters produced CNTs, the nanopearls were formed at 700 °C, with higher temperatures producing larger diameters. The product, a volumetric foam-like structure as shown in Fig. 1a, was formed only in the reaction vessel where the Ni catalysts were deposited. The volume of product formed is directly dependent on the reaction time, and the Ni nanoclusters are the key for the formation of the 3D foam-like macroscopic structure of the product. The direct growth onto surfaces of foam-like thin films of carbon nanopearls with layer thicknesses in the range of 10 μm and located at specific areas was also possible (Figs. 1b, 6a). This localized growth process was used to fabricate cold cathodes having good FE properties, the emission characteristics of which are presented in Section 5.

### 3. Characterization of the carbon nanopearls

We have performed a series of complementary analyses in order to characterize the product formed:

1. High resolution S.E.M. was used to obtain the geometrical configurations of the overall structure. Results showed strings of nanopearls organized into a 3D foam-like configuration with a sphere diameter of about 150 nm and a monodispersity estimated to about 85%. The length of the strings can be up to tens of microns, with frequent changes in the direction. Fig. 1 shows the as-grown product, illustrating the very high purity nanosphere composition without any byproducts. The foam-like macroscopic appearance of the product (Fig. 1a) can have a volume of tens of cm<sup>3</sup>. We have not determined the surface area per unit volume of these strings of nanopearls, but from the micrographs, one can expect a rather high value considering the 150-nm diameter of each unit.
2. HRTEM was used to probe the structure details within each nanopearl. These observations confirmed the spherical shape of the nanopearls and a uniform diameter ≈ 150 nm (Fig. 2). The nanopearls were connected to each other to form linear strings, with different values for the neck size diameters between adjacent nanopearls. High magnification observations indicated that the nanopearls were solid spheres composed of flakes having 2D dimension of few nanometers (2 to 6 nm) and organized in concentric layers (Fig. 2b). The interfringe distances were about 0.47 nm. Due to the flake structure, the surface of these spheres exhibits atomic corrugations corresponding to the unclosed graphitic flakes on the surface. The diffraction patterns were diffuse rings with a directional intensity enhancement (inset in Fig. 2b)

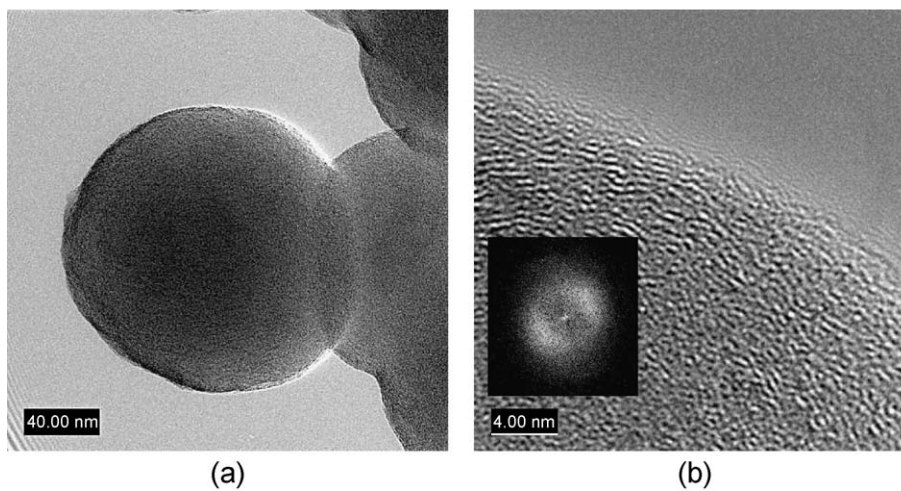


Fig. 2. HRTEM images of the carbon nanopearls. (a) A nanopearl. (b) Detail at the surface of the nanopearl. The orientation of the fringes near the surface indicates a concentric orientation of the wavy flakes. The FFT near the surface (inset) confirmed this concentric disposition. The presence of unclosed graphitic flakes at the surface can also be observed.

indicating a mixture of amorphous and oriented crystalline carbon species. The presence of nanocrystalline and disordered graphite was confirmed by Raman measurements. The spectra showed two peaks, a G-peak at  $1590\text{ cm}^{-1}$  (graphite), and a second D-peak around  $1350\text{ cm}^{-1}$  (amorphous).

3. The sizes of the graphitic crystallites were estimated from X-ray diffraction [5] (Fig. 3) and the Raman spectroscopy measurements. Using the empirical formula given by Tuinstra and Koenig [6], Raman analysis indicated a plane coherence length of about 4 nm. The mean stacking distance of the carbon layers was determined from the X-

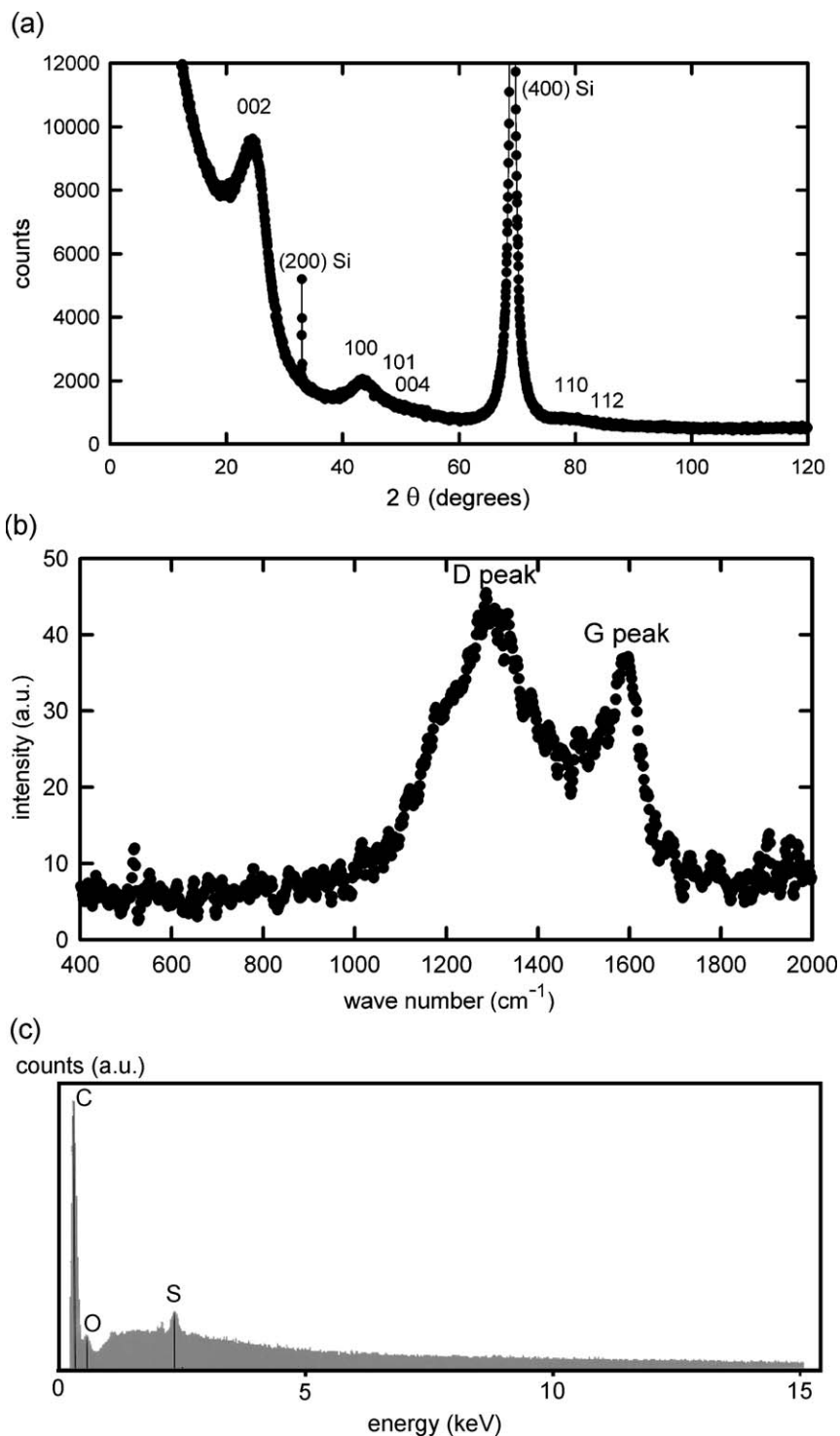


Fig. 3. (a) X-ray microdiffraction (the two peaks for Si is consequence of the use of a Si (100) wafer as the substrate for the analysis). (b) Raman (the ratio between the intensities of the G peak and the D peak gives information about the lateral dimension of the flakes). (c) X-ray fluorescence (EDX).



ray analysis by the Scherrer formula with the shape factor  $K=0.9$ , using the 002 line [7]. It showed an average size of crystallites roughly equal to 2 nm with basic cell characteristic near the values  $a=2.47 \text{ \AA}$  and  $c=6.79 \text{ \AA}$  of the conventional graphitic structure P6.mc (186), with a distortion less than 10%.

- EDX measurements were used to determine the composition of the product. These indicated mainly the presence of carbon, as expected, with traces of oxygen, silicon and sulfur. We suspect that the Si and S, as well as O, were due to contamination from the chamber and during the transfer of the samples. No traces of Ni were observed, indicating that if present its percentage concentration in the nanopearls is  $<0.1\%$ .
- In order to localize the presence of the Ni clusters within the nanopearls foam-like structure, the FPM was used. The presence of any Ni clusters will be detected by the appearance of localized Fresnel interference fringes related to its magnetic field [8]. The FPM observations of the foam-like arrangement of the carbon nanopearls indicated the presence of Ni clusters only at some rare locations. In other words, contrary to the carbon nanotubes for which one Ni cluster is always associated to each CNT, we have not seen the presence of Ni associated with each individual carbon nanopearls or strings of nanopearls. The decomposition of the acetylene into atomic carbon by the Ni nanocatalysts was then more global for the nanopearls.

#### 4. The nanopearl growth mechanism

The following steps (Fig. 4) are proposed for the growth of these nanopearls, based on the different mechanisms previously proposed [2].

- Decomposition of the acetylene into atomic carbon by the Ni nanocatalysts.
- Formation of nanosize waving flakes of graphene. The wavy 2D structure of these flakes is obtained by the combination of pentagonal and heptagonal structures with the planar hexagonal structure of graphene in order to accommodate the curvature of the carbon sphere [2].
- Aggregation in a concentric way to form the solid carbon nanospheres. As the flakes have 2D dimension in the range of 4 nm, the superposition of these flakes, concentric layer by concentric layer, will statistically create 3D nanocrystallites in the range of 2 nm, in concomitance with amorphous areas. Note that there are two possibilities for this last step, one is the formation of aggregates of the graphitic flakes before their inclusion in the concentric layers to form the carbon nanopearls and the second is the direct aggregation of individual flakes on the surface of the carbon nanopearls to form the concentric layers, then the nanocrystallites.

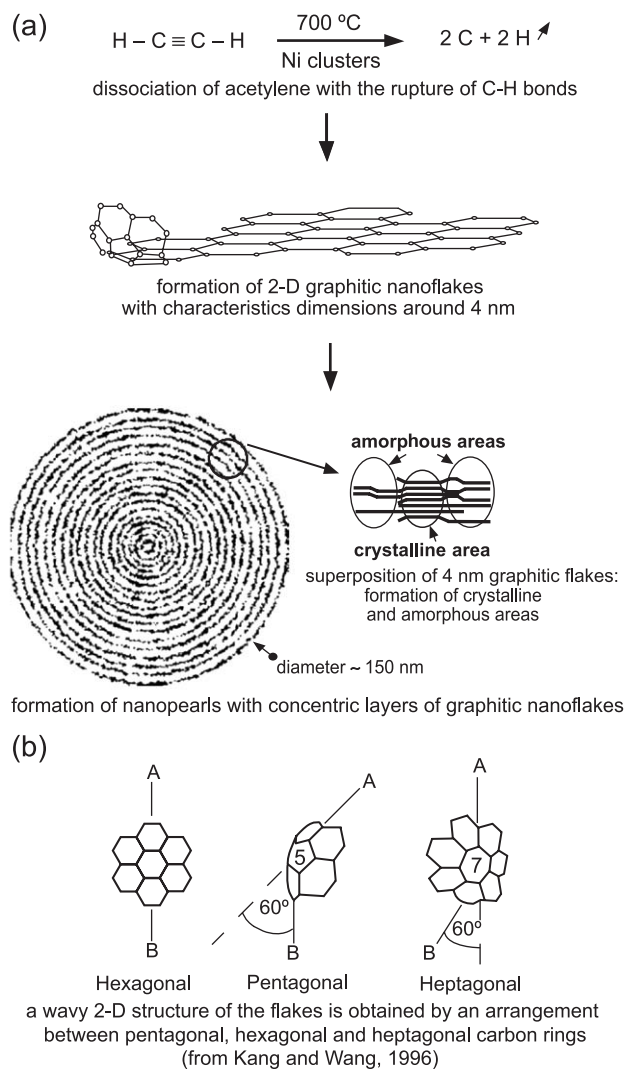


Fig. 4. (a) A schematic representation of the proposed mechanism for the formation of the carbon nanopearls in three steps. For the first step, we have no data regarding the end products formed between the various species present in the reactor, particularly the hydrogen and nitrogen. (b) Wavy flakes can be obtained by an insertion of pentagonal and heptagonal carbon rings within the planar hexagonal carbon rings.

However, there remain some aspects of the formation of these nanopearls that are not understood. The first question relates to the monodispersity of the size of the nanopearls, and the second to the formation of the string, i.e., the accretion between these nanospheres to form the string structure. Also, the exact role of the Ni nanocatalysts has to be investigated in detail.

#### 5. The nanopearls as graphitic nanostructures for field emission

Compared to other graphitic nanostructures, in particular the tubular geometry of CNTs, the nanopearls have the advantage of presenting statistically a high density of apex

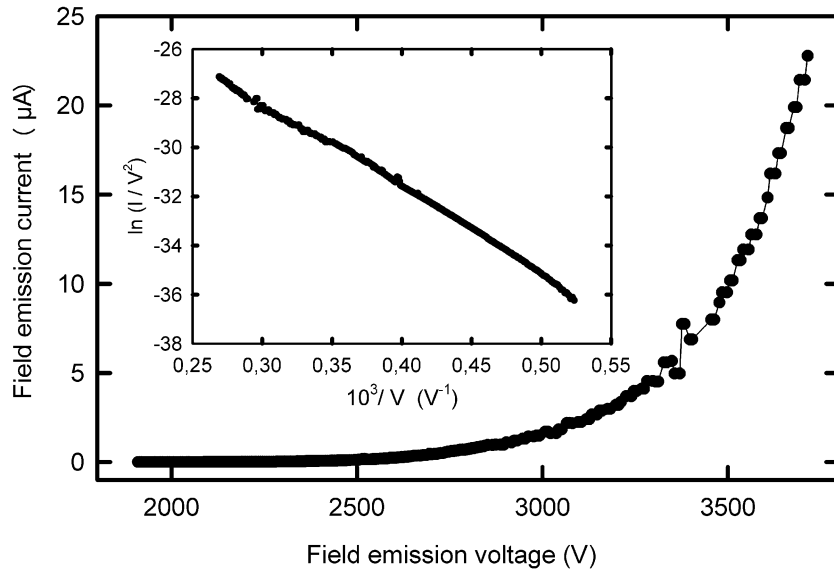


Fig. 5. An example of field emission characteristics from the foam-like arrangement of carbon nanopearls deposited directly on a metallic substrate. The  $\ln(I/V^2)$  vs.  $1/V$  plot (inset) indicates a straight line until 25  $\mu\text{A}$  total emission current. The field emission follows the conventional Fowler–Nordheim mechanism.

areas with a small radius of curvature ( $\sim 75$  nm) when deposited on a planar surface (Fig. 1c). Moreover, these spheres are composed of graphitic flakes that are unclosed at the surface (Fig. 2) and therefore believed to exhibit many dangling bonds with the potential to enhance the FE current [9]. These two properties give the nanopearls excellent prospects as a cathode material. To investigate the FE properties, we have directly grown the nanopearls on the end of a metallic wire (Fig. 1b) or a conical tip having an apex radius  $R$  (Fig. 6a). The field emission was performed in a conventional field emission microscope diode environment. The conical cathodes were located mm away from flat

screens:  $\sim 5$  mm for a fluorescent screen or less than 1 mm for a metallic anode. We used the metallic anode to measure currents over few  $\mu\text{A}$ .

Fig. 5 shows the FE current-voltage ( $I-V$ ) characteristics of these cathodes after a conditioning process. Total currents  $I$  up to 50  $\mu\text{A}$  can be obtained easily under continuous emission, and the variation with the applied voltage strictly followed conventional Fowler–Nordheim behavior, i.e. a linear variation of  $\ln(I/V^2)$  vs.  $(1/V)$ . Initially, the newly grown cathodes exhibited unstable currents, however, these instabilities were eliminated by an in situ conditioning process-heating of the cathode to about 800  $^\circ\text{C}$  and stepped

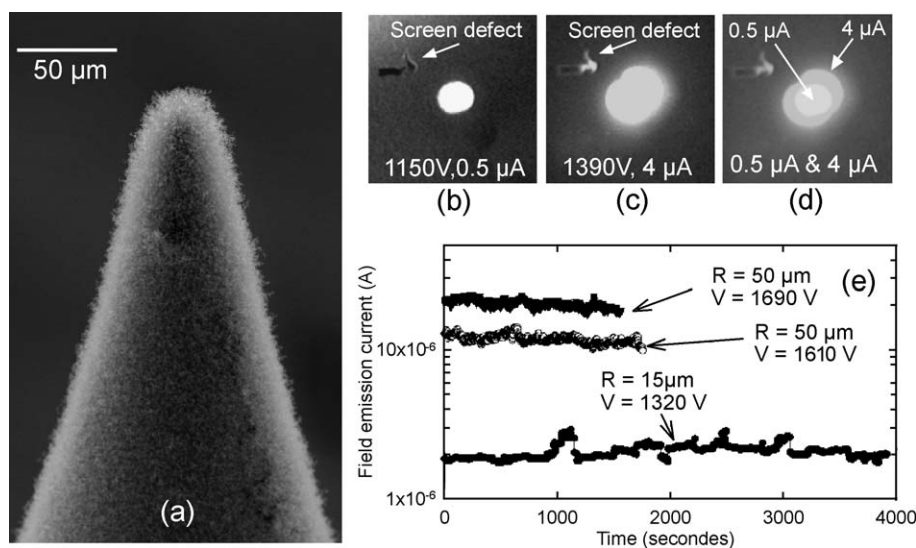


Fig. 6. (a) A characteristic cathode profile showing a uniform layer of carbon nanopearls on a metallic tip with  $R \approx 15$  Gm. (b) and (c) Characteristic FE spots on a fluorescent screen emitted from the cathode for different FE voltages. (d) The superposition of these two FE patterns indicated the increase in the emission area. (e) Characteristic stabilities of the FE currents in a vacuum of  $10^{-7}$  T. Such stability can be recorded for total duration of hours; the durations of each of these three plots, which show representative emission over arbitrary time periods, do not indicate a breakdown of the cathode.

increase of the current. Fig. 6a shows an example of a conical shape metallic tip covered with a uniform layer of foam-like nanopearls. In Fig. 6b and c, we present the FE patterns obtained from this conical tip for two FE currents (0.5 and 4  $\mu\text{A}$ ). These two figures indicate a uniformity of the FE beam and an increase of the emission area when the FE current increased. Fig. 6d is a superposition of Figs. 6b and c and illustrates this increase in the emission area. We have also plotted in Fig. 6e, the FE current stability of the same cathode for a continuous emission at 2  $\mu\text{A}$  in a vacuum of about  $10^{-7}$  Torr. The same stability was observed for higher total FE currents (at 10 and 20  $\mu\text{A}$ ) for tips having  $\sim 50$   $\mu\text{m}$  radius. For a hemispherical geometry of the conical tip cathodes, we can estimate, in a very conservative manner, the current densities by taking the emission area equal to  $\pi R^2/2$  for low FE currents and  $\pi R^2$  for high FE currents. In the example, this estimation gives  $\sim 0.15$  A/cm<sup>2</sup> for Fig. 6b and  $\sim 0.6$  A/cm<sup>2</sup> for Fig. 6c. At very high currents, some bright spots appeared at the surface of the cathode indicating that Joule heating of some nanopearl strings was occurring due to the high currents through the strings, a phenomenon that is also observed with nanotubes [10]. However, unlike CNTs, when an arc occurred at high currents in the nanopearls, any structural break-down was self-repairing and the same cathode returned to stable emission after a conditioning process, except if the whole cathode was burn-out.

## 6. Conclusions

A novel carbon nanomaterial has been synthesized using Ni nanocluster catalysis at 700 °C. The resulting carbon nanopearls are  $\sim 150$  nm in diameter with  $\sim 85\%$  mono-dispersity, with a solid nanocrystalline structure ( $\sim 2$  nm repeat units). The nanopearls form 3D strings, which give rise to a macroscopic foam-like appearance. It has been shown that a film of carbon nanopearls exhibits excellent field emission properties due to its geometry and specific surface structure. The small radius of curvature of the nanopearls, and the corrugation at the atomic scale of the

surface resulting from the unclosed graphitic flakes, were both shown to be of benefit for field emission properties, with currents up to 50  $\mu\text{A}$ , i.e., current densities in the range of 1 A/cm<sup>2</sup>, readily obtainable.

It is proposed that these nanopearl films would provide significantly higher yield, uniform emission characteristics than non-oriented films of carbon nanotubes due to the reproducibly high density of nanopearl emitter sites. However, this carbon nanomaterial is believed to have important applications in other areas such as improving the strength or electrical properties of composite materials, and the potential chemical activity of the corrugated surface suggests applications in adsorption or catalysis.

## Acknowledgements

The authors thank Dr S. Phillips and Dr. C. Esnouf for analytical support.

## References

- [1] (a) M.S. Dresselhaus, G. Dresselhaus, P.C. Eklund, *Science of Fullerenes and carbon nanotubes*, Academic Press, USA, 1996.  
(b) M.S. Dresselhaus, G. Dresselhaus, P.C. Eklund, in: P. Delhaès (Ed.), *Graphite and Precursors*, World of Carbon, vol. 1, Gordon and Breach Science Publ., NL, 2001.
- [2] Z.L. Wang, Z.C. Kang, *J. Phys. Chem.* 100 (1996) 17725–17731.
- [3] M. Sharon, K. Mukhopadhyay, K. Yase, S. Ijima, Y. Ando, X. Zhao, *Carbon* 5–6 (1998) 507–511.
- [4] V.T. Binh, A. Levesque, French patent pending, July 2003.
- [5] N. Guillon, R.Y. Fillit, *J. Phys.*, IV 8 (1998) 303–308.
- [6] F. Tuinstra, J.L. Koenig, *J. Chem. Phys. Lett.* 53 (1970) 1126–1130.
- [7] Y. Hishiyama, M. Nakamura, *Carbon* 33 (10) (1995) 1399–1403.
- [8] V.T. Binh, S.T. Purcell, V. Semet, F. Feschet, *Appl. Phys. Lett.* 72 (1998) 975–977.
- [9] (a) C. Oshima, K. Matsuda, T. Kona, Y. Mogami, M. Komaki, Y. Yamashita, T. Yamashita, T. Kuzumaki, Y. Horike, *Phys. Rev. Lett.* 88 (2002) 038301.  
(b) A. Mayer, N.M. Miskovsky, P.H. Cutler, *Phys. Rev.*, B 65 (15) (2002) 155420.
- [10] S.T. Purcell, P. Vincent, C. Journet, V.T. Binh, *Phys. Rev. Lett.* 88 (2002) 105502.